Spatial confinement controls self-oscillations in polymer gels undergoing the Belousov-Zhabotinsky reaction

Olga Kuksenok, Victor V. Yashin, and Anna C. Balazs
Chemical Engineering Department, University of Pittsburgh, Pittsburgh, Pennsylvania 15261, USA
(Received 26 September 2009; published 23 November 2009)

Chemoresponsive gels undergoing the Belousov-Zhabotinsky (BZ) reaction exhibit self-sustained pulsations, which can be harnessed to perform mechanical work. In technological applications, the gels would typically be confined between hard surfaces and thus, it is essential to establish how confinement affects these distinctive oscillations. Using theory and simulation, we pinpoint regions in phase space where the dynamic behavior of BZ gels critically depends on the presence of confining walls. We then illustrate how the wave propagation within thin samples can be tailored by selectively introducing "cut outs" in the bounding surfaces. The oscillations in the latter films are localized in specified areas, so the system contains well-defined oscillatory and nonoscillatory regions. The cut outs provide an effective means of tuning the mechanical action within the film and provide a route for tailoring the functionality of the material.

DOI: 10.1103/PhysRevE.80.056208 PACS number(s): 82.40.Bj, 82.40.Ck, 89.75.Kd

I. INTRODUCTION

The discovery of the oscillating chemical reaction known as the Belousov-Zhabotinsky (BZ) reaction [1,2] facilitated the rapid development of the field of nonlinear chemical dynamics. The temporal oscillations and spatial concentration patterns produced via this reaction provided researchers with an exceptional "laboratory" for systematically exploring systems far from equilibrium [3,4]. In an important step toward harnessing this oscillatory behavior for technological applications, Yoshida *et al.* [5–9] incorporated the BZ chemistry into responsive polymer gels and thus, for the first time, used this reaction to power a mechanical action. A vital aspect of these BZ gels is that the ruthenium catalysts are covalently bonded to the polymer chains; the BZ reaction causes Ru to undergo periodic oxidation and reduction that dynamically alter the hydrophilicity of the polymers and thereby drive the rhythmic swelling and deswelling of the gel [5–9]. Due to this mechanism, millimeter-sized gels can oscillate autonomously for hours [8] and can be "refueled" by simply adding more reactants to the surrounding solution. From a fundamental viewpoint, the BZ gels constitute a unique example of a far-from-equilibrium system where nonlinear chemical kinetics is coupled to the elastodynamics of a polymer network. In terms of practical applications, the autonomously oscillating BZ gels can provide exciting new opportunities for creating biomimetic systems that transduce chemical energy into mechanical work [9].

A scientific challenge to fully exploiting the properties of these BZ gels is to establish routes for controlling their spatiotemporal behavior so that the chemomechanical waves propagate in user-specified patterns. In this context, it is worth recalling that in many potential applications, these active gels will be localized on a surface or within a confined geometry. Thus, it is particularly important to determine how confining hard walls can be utilized to manipulate the pattern formation and yield well-defined behavior.

In previous studies, we have effectively considered the influence of uniform confining walls on one-dimensional [10] or two-dimensional systems [11]. For example, we considered a one-dimensional BZ gel, which can be viewed as a long thin sample confined within a capillary tube [10]. Through this investigation, we demonstrated that changing the sample size via stretching or compression could dramatically alter the dynamic behavior of the system. In the latter studies, the catalyst for the reaction was localized within specific patches in the polymer network, so that the BZ reaction occurred only within these patches. Moreover, the polymer network was assumed be to a nonresponsive BZ gel, i.e., it did not undergo swelling and deswelling in response to the ongoing BZ reaction.

Herein, we undertake the first studies to analyze how three-dimensional BZ gels that contain a homogeneous distribution of catalyst respond to restrictions that are imposed by bounding walls. In carrying out these investigations, we specifically focus on the responsive BZ gels. As we show below, the removal of just a portion of a wall can drive a previously stationary domain into an oscillatory state and in this manner, we can create materials with controlled arrangements of pulsatile and nonpulsatile behaviors. Thus, the results provide guidelines for tailoring the functionality of responsive self-oscillating gels. On a fundamental level, the findings reveal how the behavior of this unique nonequilibrium system, which encompasses coupled chemical and mechanical degrees of freedom, is affected by confinement.

II. METHODOLOGY

To simulate the dynamics of the BZ gels, we utilize our recently developed computational approach for capturing the three-dimensional behavior of these complex materials [12]. Via this approach, we obtained qualitative agreement between our results and various experimental findings [12]; in particular, for small samples, we observed the in-phase synchronization of the chemical and mechanical oscillations [7]. We also recover the decrease of the oscillation period with an increase in the concentration of one of the substrates [6].

Our model is formulated in terms of the volume fraction of polymer, ϕ, and the dimensionless concentrations of the dissolved reagent, u, and oxidized metal-ion catalyst, v. The

governing evolution equations can be written as [13]

$$\frac{d\phi}{dt} = -\phi \nabla \cdot \mathbf{v}^{(p)}, \tag{1}$$

$$\frac{dv}{dt} = -v \nabla \cdot \mathbf{v}^{(p)} + \varepsilon G(u,v,\phi), \tag{2}$$

$$\frac{du}{dt} = -u \nabla \cdot \mathbf{v}^{(p)} + \nabla \cdot \left[\mathbf{v}^{(p)} \frac{u}{1-\phi} \right] + \nabla \cdot \left[(1-\phi) \nabla \frac{u}{1-\phi} \right] + F(u,v,\phi). \tag{3}$$

Here $\frac{d}{dt} \equiv \frac{\partial}{\partial t} + \mathbf{v}^{(p)} \cdot \nabla$ denotes the material derivative associated with the polymer velocity, $\mathbf{v}^{(p)}$. We assume [13] that it is solely the polymer-solvent interdiffusion that contributes to the gel dynamics and neglect the total velocity of the polymer-solvent system [14], so that $\phi \mathbf{v}^{(p)} + (1-\phi)\mathbf{v}^{(s)} \equiv 0$, where $\mathbf{v}^{(s)}$ is the solvent velocity. The functions $G(u,v,\phi)$ and $F(u,v,\phi)$ are based on the Oregonator model for BZ reactions in solution and are [13,15]

$$F(u,v,\phi) = (1-\phi)^2 u - u^2 - (1-\phi) f v \frac{u - q(1-\phi)^2}{u + q(1-\phi)^2}, \tag{4}$$

$$G(u,v,\phi) = (1-\phi)^2 u - (1-\phi) v. \tag{5}$$

The stoichiometric factor f and the dimensionless parameters ε and q have the same meaning as in the original Oregonator model.

The dynamics of the polymer network is assumed to be purely relaxational. Consequently, the constitutive equation for the BZ gel can be written as [13]

$$\hat{\boldsymbol{\sigma}} = -P(\phi,v)\hat{\mathbf{I}} + c_0 v_0 \frac{\phi}{\phi_0} \hat{\mathbf{B}}. \tag{6}$$

Here, $\hat{\mathbf{I}}$ is the unit tensor, $\hat{\mathbf{B}}$ is the strain tensor, and the pressure $P(\phi,v)$ is defined as

$$P(\phi,v) = \pi_{osm}(\phi,v) + c_0 v_0 \phi / 2\phi_0, \tag{7}$$

with the contribution from the osmotic pressure of the polymer being [13]

$$\pi_{osm} = -[\phi + \ln(1-\phi) + \chi(\phi)\phi^2] + \chi^* v \phi, \tag{8}$$

where $\chi(\phi) = \chi_0 + \chi_1 \phi$ is the polymer-solvent interaction parameter [16] and the constant $\chi^* > 0$ couples the gel dynamics to the chemical reaction [15,17]. The gel's degree of swelling is given by $\lambda = (\phi_0/\phi)^{1/3}$. We numerically solve the above equations via our recently developed 3D gel lattice spring model [12]; we apply no flux boundary conditions for u on sample's surface [12].

III. RESULTS AND DISCUSSION

To begin, we focus on the scenario shown in Fig. 1, where a cubic gel sample is initially bound by hard walls on all sides. (In the simulations, such confinement is implemented by fixing the positions of all the surface nodes). For the chosen parameters, the confined BZ gel is in the nonoscillatory stationary state [Fig. 1(a)]. At time $t \equiv t_0$, however, we remove the confinement (i.e., allow the surface nodes to move) and find that this release induces nondecaying chemomechanical oscillations [Figs. 1(b)–1(d)]. In other words, by simply lifting the confining surfaces, we can drive the system from the steady state into the oscillatory regime.

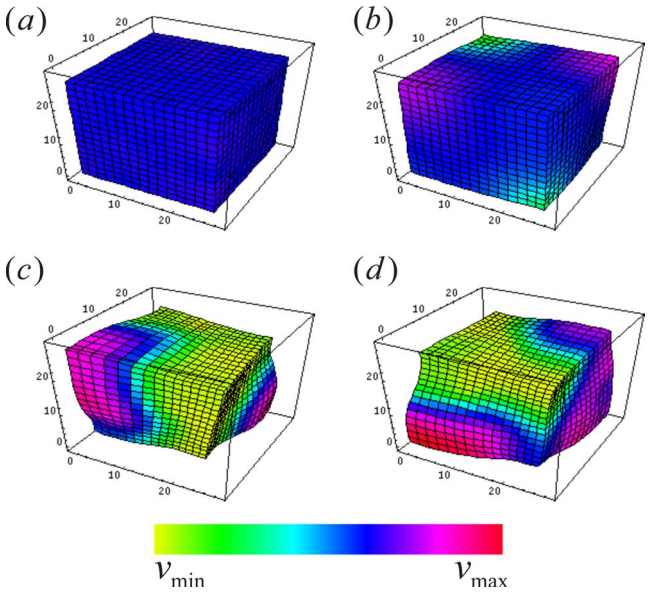

FIG. 1. (Color online) (a) Confined gel sample (i.e., positions of all the surface nodes are held fixed). (b)–(d) Sample after the confinement is removed. Chemomechanical oscillations at times $t=154$, 300, and 306, respectively. Sample size is $16\times16\times16$ nodes, $f=0.76$ and $\varepsilon=0.7$. All other parameters (unless specified otherwise) are the same as in Ref. [11]. With this choice of parameters, the characteristic time and length scales in our simulations are ~ 1 s and ~ 40 μm, respectively [16]. The color bar in (d) indicates the concentration of oxidized catalyst, with $v_{min}=2\times10^{-4}$ and $v_{max}=0.35$.

To determine the generality of this effect, we first isolate the critical parameters where the stationary solutions become unstable for the two simplest limiting cases (cases A and B defined below). We then extend our studies to understand the dynamic behavior in a number of more complex scenarios.

Case A. For sufficiently small sample size and high polymer mobility, we can neglect the contributions from diffusion in Eq. (3) and assume that the evolution of ϕ follows the changes in the reactant concentrations. The latter assumption means that the elastic stress is instantaneously equilibrated with the osmotic pressure, i.e.,

$$c_0 v_0 [(\phi/\phi_0)^{1/3} - \phi/2\phi_0] = \pi_{osm}(\phi,v). \tag{9}$$

From Eq. (9), we obtain the concentration of the oxidized catalyst in this limiting case,

$$v_{lim}(\phi) = (\phi\chi^*)^{-1}[c_0 v_0 [(\phi/\phi_0)^{1/3} - \phi/2\phi_0] + \ln(1-\phi) + \phi + (\chi_0 + \chi_1\phi)\phi^2].$$

Then, we find u and ϕ from

$$\frac{d\phi}{dt} = \frac{\phi}{v_{\lim}(\phi)}\left[\frac{dv_{\lim}(\phi)}{dt} - \varepsilon G|_{v=v_{\lim}(\phi)}\right], \tag{10}$$

$$\frac{du}{dt} = -\frac{u}{1-\phi}\frac{d\phi}{dt} + F|_{v=v_{\lim}(\phi)}. \tag{11}$$

Using the above expression for $v_{\lim}(\phi)$, the right-hand sides of Eqs. (10) and (11) become $R_\phi = c(\phi,u)/b(\phi)$ and

$$R_u = u[(1-\phi)^2 - u] + f[a(\phi)(1-\phi)/2\phi\phi_0\chi^*] \times \{[(1-\phi)^2 q - u]/[(1-\phi)^2 q + u]\} - [u/(1-\phi)] \times [c(\phi,u)/b(\phi)],$$

respectively. Here,

$$a(\phi) = c_0[-\phi + 2\phi^{1/3}\phi_0^{2/3}] + 2\phi_0[\phi + \phi^2(\chi_0 + \chi_1\phi) + \ln(1-\phi)],$$

$$b(\phi) = c_0(1-\phi)[10\phi^{1/3}\phi_0^{2/3} - 3\phi] + 6\phi_0[2\phi - \phi^2[1 + \chi_1(1-\phi)\phi] + 2(1-\phi)\ln(1-\phi)],$$

and

$$c(\phi,u) = 3\varepsilon(1-\phi)^2\phi[a(\phi) - 2(1-\phi)\phi\phi_0 u\chi^*].$$

We find the stationary solution $\{u_{st}, \phi_{st}\}$ of Eqs. (10) and (11) by solving $G|_{v=v_{\lim}(\phi)}=0$, $F|_{v=v_{\lim}(\phi)}=0$ [18]. To analyze the stability of the solution $\{u_{st}, \phi_{st}\}$, we linearize Eqs. (10) and (11) with respect to small fluctuations and find the growth rate of the fluctuations, $p_{1,2}=(T \pm \sqrt{T^2-4D})/2$ (here, $T=[\partial_u R_u + \partial_\varphi R_\varphi]|_{\{u_{st}\phi_{st}\}}$, $D=[\partial_u R_u \partial_\varphi R_\varphi - \partial_\varphi R_u \partial_u R_\varphi]|_{\{u_{st},\phi_{st}\}}$, and $\partial_u \equiv \partial/\partial u$).

Case B. Another limiting case is one where the entire sample is constrained, namely, where all the faces of the 3D sample are attached to hard walls so that the volume of the sample remains constant. Again, we consider a small sample and neglect diffusion in Eq. (3). Here, we fix $\phi \equiv \phi_{st}$, so that the dynamics is described solely by Eqs. (2) and (3) with $\phi \equiv \phi_{st}$ [19].

Figure 2(a) provides the stability map for cases A (solid line) and B (dashed line) in terms of the important variables of the BZ reaction, f and ε; recall that f characterizes the stoichiometry of the reaction and ε is proportional to the concentration of malonic acid. This map indicates the critical values of $f \equiv f^c$ where the stationary solution is no longer stable for the A and B cases; plots for responsive gel ($\chi^*=0.105$) are in light gray (red online) and for a less responsive sample ($\chi^*=0.05$) are in dark gray (blue online). If the values of $\{f,\varepsilon\}$ lie below the respective solid curves, the sample remains in the steady state whether or not it is attached to hard walls. If, however, the $\{f,\varepsilon\}$ values are above the respective dashed curves, the sample undergoes oscillations (chemomechanical in case A and purely chemical in case B since the mechanical oscillations are suppressed by fixing the sample's size). Note that f_c increases with increasing ε.

The most interesting behavior, however, is observed when the parameters are located between the solid and dashed curves. Here, the behavior of the sample dramatically depends on whether or not it is confined: the sample oscillates when it is free and remains in the stationary state when it is attached to the bounding surfaces. Figure 2(a) further reveals that the size of this region increases with increases in ε and is larger for the more responsive sample (red curves). Figure 2(b) shows that the effect is robust for a large range of cross-link densities; however, the size of the region between the solid and dashed curves only weekly depends on the value of c_0.

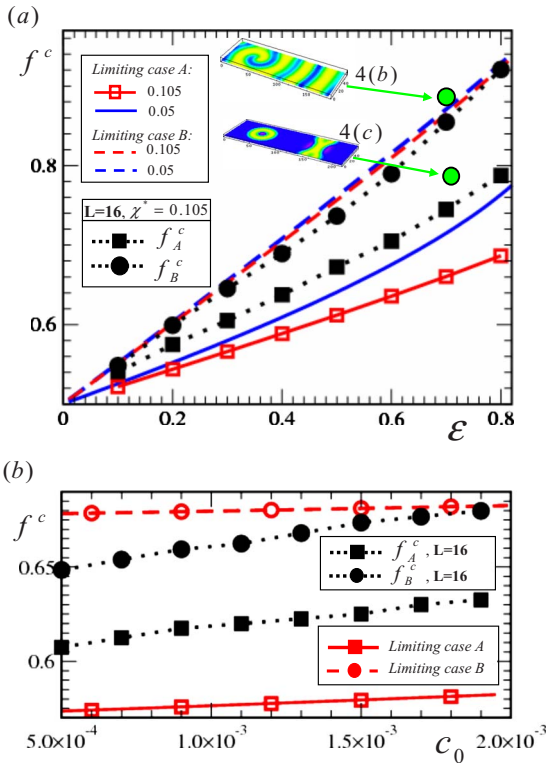

FIG. 2. (Color online) Dependence of f^c on ε in (a) and on c_0 in (b). For $f > f_c$, the steady state solution is unstable. Curves for the limiting cases A (solid) and B (dashed) are shown in red (light gray) for $\chi^*=0.105$ and in blue (dark gray) for $\chi^*=0.05$ [in (a) only]. Simulation results for the sample of size $L\times L\times L$ nodes with $L=16$ are shown in black, with the simulation points marked by filled squares for the free sample (f_A^c) and filled circles for the constrained sample (f_A^c).

For cases A and B, our simulations are in excellent agreement with the linear stability analysis, as can be seen in Fig. 2 where the open symbols mark the simulation points [20]. However, for larger samples, where diffusion of the reagent can no longer be neglected (and the mobility of polymer network has a finite value), the analogous analytical analysis is prohibitive and we must turn to the simulations to determine the properties of the system. Consequently, we ran simulations for a sample of size $L\times L\times L$ with $L=16$ nodes [i.e., a dimensionless linear size of $(L-1)\lambda_{st}$], $\chi^*=0.105$, and a range of f values (taken at intervals of $\Delta f = 2.5\times10^{-2}$). In Fig. 2(a), we plot the critical values of f that correspond to the transitions between the stationary and the oscillatory states for this larger sample when it is free (solid squares) or confined on all sides (solid circles). The interconnecting dotted lines define the corresponding regions in the

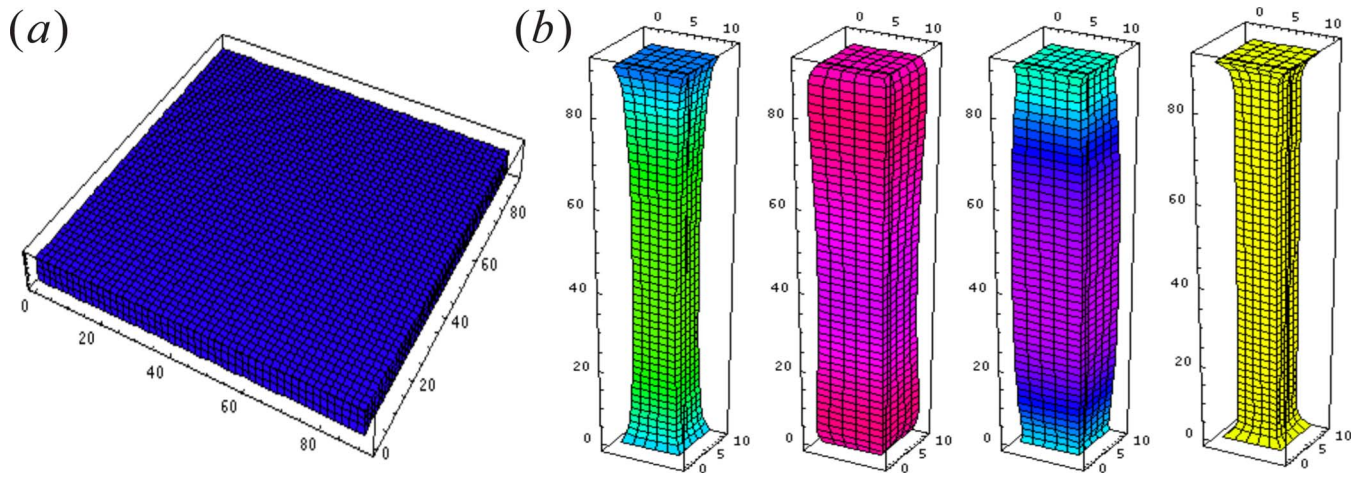

FIG. 3. (Color online) Gels confined at the top and bottom surfaces; sample sizes are $50\times50\times4$ nodes in (a) and $6\times6\times50$ nodes in (b). Simulation times in (b) are $t=6900$, 6906, 6912, and 6924 (from left to right). The other parameters are the same as in Fig. 1.

phase maps; we mark these lines as f_A^c and f_B^c for the cases of the free and constrained samples, respectively. Clearly, the region where the effects of the confinement are the most dramatic ($f_A^c<f<f_B^c$) is narrower for these large samples than the smaller gels (marked in red). The effect of confinement in this region, however, remains similar to the one observed in limiting cases. Namely, the sample continues to be in the stationary state as long as its sidewalls are held fixed and undergoes oscillations when the confinement is removed. This behavior was illustrated in Fig. 1, where we chose parameters in the middle of the $f_A^c<f<f_B^c$ region.

In general, the exact values of f_B^c, f_A^c will depend on the actual dimensions of the sample. However, the results of the linear stability analysis for the two simplest examples and the simulation results for the larger cubic samples provide us with approximate guidelines for predicting the behavior of various cases. Namely, if we select an f in the middle of the region $[f_A^c,f_B^c]$, we anticipate that the free sample of *any size* will oscillate, but a bounded sample will remain stationary. We emphasize that this statement is valid for samples where *all* the faces are either free or confined. We can, however, also use the information in Fig. 2 to design the dynamic properties of BZ gels by partially confining of the samples, i.e., by bounding only some portions of the sample's surfaces.

To illustrate the above point, we first consider scenarios where only the top and bottom faces are held fixed and the rest of the sample is unrestricted (see Fig. 3). We choose different dimensions of the sample but keep the same physical parameters of the system; here, we set $f=0.76$ and $\varepsilon=0.7$ (in the middle of the $[f_A^c,f_B^c]$ region in Fig. 2(a)). In the limit of small sample thickness, one expects this gel film to behave similarly to case B (where the entire sample was constrained). Indeed, the sample in Fig. 3(a) remains in the stationary state as long as its top and bottom faces are held fixed. We now alter the gel's dimensions, making the sample thin and long in the z direction [see Fig. 3(b)]. In contrast to the case in Fig. 3(a), the majority of the sample is now unconstrained; hence, we anticipate its behavior to be similar to a nonconfined sample. Figure 3(b) confirms this prediction, showing two traveling waves that are generated at the top and bottom walls; these waves propagate and collide at the center of the sample [21].

Finally, we turn our attention to examples of nonuniform confinement; we consider thin samples that are attached to hard walls everywhere except two specific regions, which are marked by a white circle of radius R_0 and a rectangle with width W_0 [see Fig. 4(a)]. We choose the value of f higher than f_B^c for the case in Fig. 4(b) and within the region $[f_A^c,f_B^c]$ for the case in Fig. 4(c). [The selected $\{f,\varepsilon\}$ are marked in Fig. 2(a).] In Fig. 4(b), a traveling wave propagates throughout the sample, with only small distortions caused by the presence of the free regions. The situation is dramatically different, however, in Fig. 4(c), where the oscillations are observed only within the free regions, while the regions that are held fixed remain in the stationary state [22]. Thus, one film contains well-defined regions of both oscillatory and nonoscillatory behaviors.

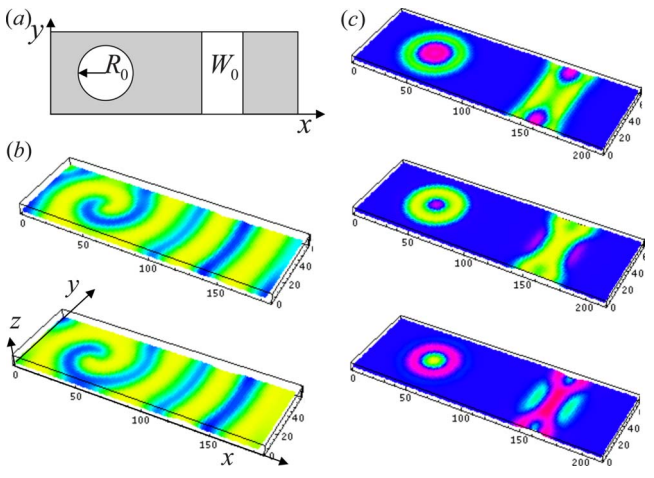

FIG. 4. (Color online) (a) Schematic of the sample (top view). White areas are unbounded within the top and bottom surfaces. Sample size is $120\times40\times2$ nodes; $R_0=17$ and $W_0=20$ nodes and the separation between the centers is 60 nodes. (b) $f=0.88$, and times are $t=3900$ and 3906. (c) $f=0.78$, and times are $t=3912$, 3918, and 3930 (from top to bottom).

Figure 4(c) reveals that "cut outs" in the confining surfaces provide an effective means of controlling the oscillations of active BZ gels and hence the functionality of the material. Different arrangements or shapes of these cut outs can be utilized to produce different dynamic behaviors. For this reason, the phase map in Fig. 2 is particularly valuable since it identifies useful parameters for creating films with distinct pulsations in an otherwise stationary layer.

IV. CONCLUSIONS

In summary, we determined regions in parameter space where the dynamic behavior of BZ gels can be altered by the introduction or removal of confining walls. This behavior opens up opportunities for harnessing the gels for novel technological applications. For example, the oscillations induced by the unintentional removal of a surface could be used as an indicator, signaling that the structural integrity of a system has been compromised. Furthermore, the intentional release of a confined sample—or just a portion of the sample—provides a means of tuning the mechanical action of the system. Hence, by manipulating the nature of the confinement, one can not only tailor the functionality of these systems but also impart new functionality into active biomimetic devices.

ACKNOWLEDGMENTS

The authors gratefully acknowledge financial support from ARO.

[1] B. P. Belousov, *Collection of Short Papers on Radiation Medicine* (Medgiz, Moskow, 1959).
[2] A. N. Zaikin and A. M. Zhabotinsky, Nature (London) **225**, 535 (1970).
[3] I. R. Epstein and J. A. Pojman, *An Introduction to Nonlinear Chemical Dynamics: Oscillations, Waves, Patterns, and Chaos* (Oxford University Press, New York, 1998).
[4] T. Sakurai *et al.*, Science **296**, 2009 (2002).
[5] R. Yoshida *et al.*, J. Am. Chem. Soc. **118**, 5134 (1996).
[6] R. Yoshida *et al.*, J. Phys. Chem. A **103**, 8573 (1999).
[7] R. Yoshida *et al.*, J. Phys. Chem. A **104**, 7549 (2000).
[8] S. Sasaki *et al.*, Langmuir **19**, 5595 (2003).
[9] R. Yoshida, Bull. Chem. Soc. Jpn. **81**, 676 (2008).
[10] V. V. Yashin, K. J. Van Vliet, and A. C. Balazs, Phys. Rev. E **79**, 046214 (2009).
[11] O. Kuksenok, V. V. Yashin, and A. C. Balazs, Soft Matter **3**, 1138 (2007).
[12] O. Kuksenok, V. V. Yashin, and A. C. Balazs, Phys. Rev. E **78**, 041406 (2008).
[13] V. V. Yashin and A. C. Balazs, J. Chem. Phys. **126**, 124707 (2007).
[14] B. Barriere and L. Leibler, J. Polym. Sci., Part B: Polym. Phys. **41**, 166 (2003).
[15] V. V. Yashin and A. C. Balazs, Macromolecules **39**, 2024 (2006).
[16] S. Hirotsu, J. Chem. Phys. **94**, 3949 (1991).
[17] V. V. Yashin and A. C. Balazs, Science **314**, 798 (2006).
[18] We use this solution $\{u_{st}, \phi_{st}, v_{st} \equiv v_{\mathrm{lim}}(\phi_{st})\}$ with small random fluctuations of the reagent concentrations around their stationary values as initial conditions in all the simulations.
[19] If the constrained sample was initially stretched or compressed (i.e., $\phi \neq \phi_{st}$), the boundaries of the stability domain on the phase diagram should be altered. The effect of stretching or compressing the sample on behavior of heterogeneous BZ gels was studied earlier for the one-dimensional case (see Ref. [10]), and the effect of uniform compression on the dynamics of homogeneous two-dimensional samples was considered in Ref. [11].
[20] For the limiting cases in Fig. 2, simulation points are shown only for some of the curves to maintain the clarity of the image. We have, however, confirmed excellent agreement between the simulations and analytical results for all the curves in the limiting cases.
[21] If we remove one of the walls, we observe that the traveling wave is generated at the fixed end and propagates to the free end, consistent with the experimental observations for similar samples [R. Yoshida *et al.*, Chaos **9**, 260 (1999)] and with simulations of 2D BZ gel films [13].
[22] To observe such oscillations within the free regions, the sizes R_0 and W_0 must exceed some critical values. Additional simulations show that for the case in Fig. 4(c), these critical values are $R_0=5$ and $W_0=7$ nodes. These values also depend on the sample thickness, as well as the actual values within the $[f_{\mathrm{A}}^c, f_{\mathrm{B}}^c]$ region. For example, as one might anticipate, it becomes more difficult to induce oscillations if we choose parameters closer to the lower curve, f_{A}^c.